DOI: 10.1002/ejoc.201101008

How Space-Filling Is a Pyridine Lone Pair?

Andrea Mazzanti,*[a] Lodovico Lunazzi,[a] Susan Lepri,[b] Renzo Ruzziconi,*[b] and Manfred Schlosser*[c]

Keywords: Steric hindrance / NMR spectroscopy / Biaryls / Density functional calculations / Torsional energy diagrams

The torsional barriers of 2′-substituted 2-arylpyridines have been probed experimentally (by using dynamic NMR spectroscopy) and computationally (by using density functional theory). Due to the compressibility of the lone pair, the torsional barriers of the arylpyridines are up to 4.2 kcal/mol smaller than those of the carba-analogous biphenyls. Furthermore, the ground states of the 2-arylpyridines are less twisted than those of the biphenyls. Finally, due to an out-of-collinearity distortion, the intramolecular repulsion is attenuated in both rotational transition states, in the *syn* coplanar conformer (in which the pyridine nitrogen and the substituent R face each other) and in the *anti* coplanar conformer (in which they are on opposite sides of the molecule).

Introduction

The space requirements of a naked proton being negligible, a priori no major difference should exist between the size of the lone pair at a carbanionic center and the C–H bond resulting from its protonation. In both cases, it is a doublet of electrons that fills the spatial volume. The same reflections apply to the isoelectronic comparison between the lone pair residing on the nitrogen atom of an amine and the corresponding $^{+}$N–H bond. However, the electron density contours differ. Lone pairs will surround their only poles of attraction, be it nitrogen or negatively charged carbon, as spherically as possible.[1,2] In contrast, a C–H or $^{+}$N–H bond is more slender and elongated as the binding electron pairs are tightly held between two nuclei.[1,2] Therefore, whatever experimental test is applied, the lone pair proves to be "smaller" than the bond resulting from its protonation. The difference is considerable if one refers to Charton's set of υ (upsilon)[3] parameters. Although being derived from van der Waals radii,[4] they almost coincide with Taft's kinetically based E_s values.[5] Charton's scale ranks the amino entity (υ^{NH_2} = 0.35) substantially below the ammonium group (υ^{+NH_3} = 0.49), the υ parameter of which is almost identical with that of a methyl group (υ^{CH_3} = 0.52).

[a] Department of Organic Chemistry "A.Mangini", University of Bologna, Viale Risorgimento 4, 40136 Bologna, Italy Fax: +39-051-2093654 E-mail: andrea.mazzanti@unibo.it
[b] Chemistry Department, University of Perugia, Via Elce di Sotto 10, 06100 Perugia, Italy E-mail: ruzzchor@unipg.it
[c] Institute of Chemical Science and Engineering, Ecole Polytechnique Fédérale (EPFL-BCh), 1015 Lausanne, Switzerland E-mail: manfred.schlosser@epfl.ch

Supporting information for this article is available on the WWW under http://dx.doi.org/10.1002/ejoc.201101008.

The torsional barriers of methylamine and ethane (having H–N–H and H–C–H bond angles of 107.1[6,7] and 107.7°[8]) amount to 1.96[9] and 2.88 kcal/mol,[10] respectively. The piperidine invertomer, in which the lone pair occupies the equatorial as opposed to the axial position, is energetically favored by just 0.36 kcal/mol[11] (by 0.40 kcal/mol according to force-field calculations[12] or by a still moderate 0.74 kcal/mol according to a reinvestigation[13]).

According to a recent DFT calculation,[14] 2-phenylpyridine has a significantly smaller twist angle of 21° than biphenyl (44°[15–17]) and the energy it requires to attain the coplanar structure, the transition state of the aryl–hetaryl rotation, is lower (E_{tors} = 1 kcal/mol[14]) than that reported for the carba-analogous biphenyl ($E_{tors} \approx$ 2 kcal/mol[17,18]). Assuming the additivity of two repulsive interactions, experimental findings[19] can be extrapolated to an estimate of 1.2 kcal/mol for the 2-phenylpyridine torsional barrier. With other topologies, it is not always easy to predict the space requirements of pyridines relative to benzenes. This can be deduced from the landmark work of Boekelheide, Vögtle, and Nozaki and their co-workers[20–23,29,30] (Table 1).

The flip barrier[20,21] of 2,6-*ansa*-pyridines is, in the case of a heptamethylene chain, only moderately smaller than that of the carba-analogous biphenyl (9.0 vs. 11.5 kcal/mol for Z = N and CH, respectively; Table 1).[22,23] Also, in the case of some metaparacyclophanes containing two CH_2SCH_2 links between the two aryl rings, the differences are quite small.[24,25]

However, the activation energies vary by more than 10 kcal/mol when a 2,6-pyridinediyl or a 1,3-phenylene ring is incorporated into the oligomethylene chain (14.8 vs. >27 kcal/mol; Table 1)[26,27] and by at least 7 kcal/mol for the dithia analogues (<13.6 vs. 20.5 kcal/mol; Table 1).[27] Finally, the ring inversion of parametacyclophane and its

Table 1. Comparison of the ring-flip activation energies of 1,3-*ansa*-benzenes (Z = CH) with those of 2,6-*ansa*-pyridines (Z = N).

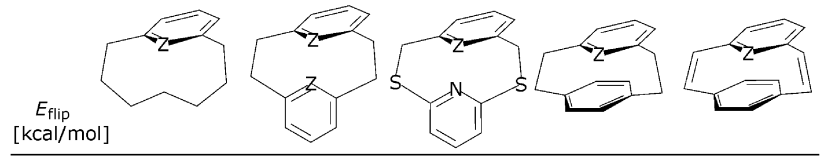

E_{flip} [kcal/mol]					
Z = CH	11.5	>27	20.5	20.6	8.3
Z = N	9.0	14.8	<13.6	10.7	0.0[a]

[a] The ground state has a different symmetry, so there is no flip barrier. See ref.[30]

diene (20.6 and 8.3 kcal/mol, respectively; Table 1) is impeded by barriers that surpass those encountered for the corresponding pyridine compounds, again by nearly 10 kcal/mol (Table 1).[28–30]

The torsional barriers of *ortho*-substituted biphenyls represent reliable criteria for scaling steric bulk.[31] Up to now, such "*B* values" have been determined for more than two dozen substituents.[31–33] The measurements were accomplished by variable-temperature ("dynamic") NMR spectroscopy, monitoring the flip of the axially chiral biphenyl conformer into its mirror image by means of diastereotopicity probes such as an isopropyl,[34] isopropyldimethylsilyl,[31] or hexafluoro-α-hydroxyisopropyl[32] group located at the 3′-position.[35]

Results and Discussion

It was deemed instructive to apply this technique to a series of 2-arylpyridines to compare the effective size of the pyridine lone pair with a transparent model system. The selected congeners of 2-phenylpyridine (**1**) carried a methyl (**2**), ethyl (**3**), isopropyl (**4**), and *tert*-butyl (**5**) group at the 2′-position. Harboring magnetically nonequivalent nuclei, ethyl- and isopropyl-substituted compounds are self-monitoring. An isopropyldimethylsilyl diastereotopicity probe was nevertheless attached to the 4-position of all the 2-arylpyridines except in the case of the isopropyl-substituted compound[35] (Scheme 1).

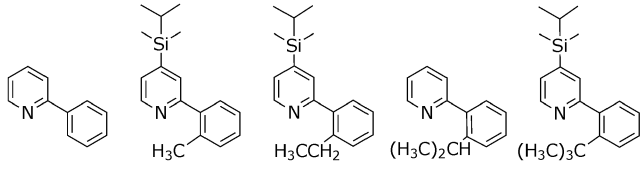

Scheme 1. Model compounds **1**–**5** employed to probe the barriers to rotation of 2-arylpyridines.

The synthesis of the samples **2**–**5** was straightforward. It relied on the well-established addition of organolithium to the corresponding pyridine followed by the re-aromatizing elimination of lithium hydride (for details see the Exptl. Sect.).[36,37]

In view of the minute torsional barrier,[14] there was no chance of freezing out the rotation about the central axis of a diastereotopically 4-labeled 2-phenylpyridine,[38] not even at –173 °C (100 K). At temperatures as low as this, the 2-(*o*-tolyl)pyridine derivative **2** did not show decoalescence either. The torsional barriers of compounds **1** and **2**, shown in parentheses in Table 2, were obtained by computation. In contrast, the signals of the diastereotopic nuclei of model compounds **3**–**5** broadened upon cooling and eventually split into two separate peaks.

Table 2. Experimental and computational torsional energies[a] ($\Delta G^{\neq}$) for the 2-arylpyridines **1**–**5** and, for comparison, the carba-analogous biaryls.

Compound	R	$\Delta G^{\neq}$ [kcal/mol]	
		Z = N	Z = CH[b]
1	H	(1.0)[c]	(2.0)[d]
2	CH_3	(3.1)[e]	7.4[e]
3	CH_2CH_3	5.9[f]	8.6
4	$CH(CH_3)_2$	6.9[f]	11.1[e]
5	$C(CH_3)_3$	11.6[f]	15.5[e]

[a] Calculated energies are given in parentheses. [b] Ref.[34a] [c] Ref.[14] [d] Ref.[17] [e] Present work: determined by B3LYP/6-311++G(2d,p) calculations of the compound without the substituent at the 4-position. [f] Present work: experimental (NMR) data.

In particular, the diastereotopicity of compound **3** was detected by the observation, at a very low temperature (–160 °C), of two ^{1}H lines for the silicon-bonded methyl groups of the *i*PrMe$_2$S substituent as well as of two ^{1}H signals for the two geminal hydrogen atoms of the ethyl group. The shift separation of the latter signals (99 Hz at 600 MHz) was much larger than that of the Me$_2$Si lines (19 Hz) and this larger value allowed us to obtain a very accurate line-shape simulation (see Figure 1), which gave a $\Delta G^{\neq}$ value (5.9 kcal/mol, Table 2) with an uncertainty as small as ±0.1 kcal/mol.

The torsional barriers determined by line-shape analysis of the 2′-ethyl-, 2′-isopropyl-, and 2′-*tert*-butyl-substituted 2-phenylpyridines (**3**–**5**) are lower than the values of the carba-analogous biphenyls by 2.7–4.2 kcal/mol (Table 2). Thus the incorporation of an imine nitrogen into the 2-position of a 2′-substituted biphenyl diminishes the torsional barrier of the latter significantly. In this sense, the lone pair of a pyridine nitrogen atom is without doubt "smaller" or,

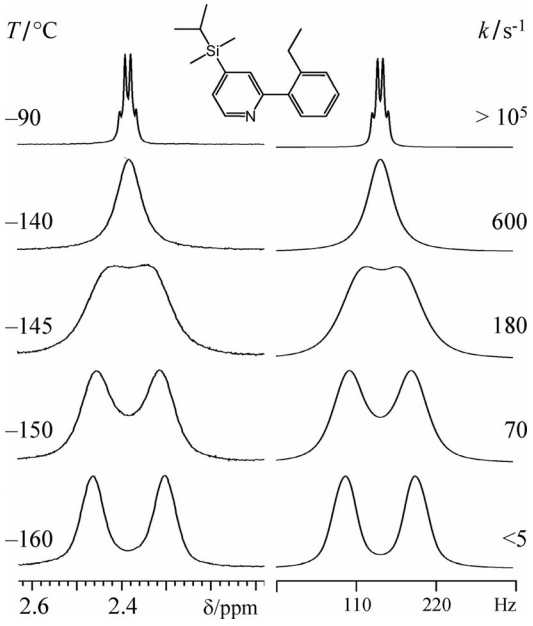

Figure 1. Temperature dependence of the ^{1}H NMR signal (600 MHz in $CHF_2Cl/CHFCl_2$) of the CH_2 group of compound **3** (left). On the right, spectra simulated with the rate constants *k*.

more accurately termed, more deformable than an aromatic C–H bond.

The numbers extracted from the variable-temperature NMR spectra represent free energy differences between the conformational ground and transition states. They do not tell us anything about the pertinent structures. Extensive quantum chemical calculations at the B3LYP/6-311++G(2d,p) level of theory provided this information (all calculations of compounds **2**, **3**, and **5** ignore the diastereotopicity probe at the 4-position).[35]

As expected, the 2-arylpyridines **2**–**5** are found to be twisted (skewed). However, their dihedral angles are considerably smaller than those of their carba-analogues (see Table 3). The big difference in the twist angles of the parent compounds 2-phenylpyridine (21°[14]) and biphenyl (45°[15,16]) has previously been recognized.

Table 3. Twist angles of the *syn*- and *anti*-skew 2-arylpyridine ground states and those of the carba-analogous biaryls.

Compound	R	Twist angle [°]	
		Z = N[a]	Z = CH[b]
1	H	21	45
2[c]	CH_3	48;136	61
3[c]	CH_2CH_3	52;124	68
4	$CH(CH_3)_2$	53;128	61
5[c]	$C(CH_3)_3$	69[d]	90

[a] Twist angles of *syn*- and *anti*-skew conformations of the 2-arylpyridines (first and second number, respectively). [b] Twist angle of 2-R-biphenyl. [c] Calculations of the corresponding compounds without the diastereotopicity probe at the 4-position [B3LYP/6-311++G(2d,p) level]. [d] The *anti*-skew conformation of **5** does not correspond to an energy minimum.

The infinite manifold of 2-aryl conformations encompasses two extreme geometries. Both of these represent transition states in the free-energy diagrams (Scheme 2). The structure locking the aryl and pyridyl rings in a perpendicular position marks the transition state for the "wagging motion" that equilibrates the twisted ground state of 2-phenylpyridine with its mirror image. Because the corresponding barrier is very low (about 1 kcal/mol), only time-averaged spectra were recorded, even at –160 °C. The coplanarity of the two rings is the other extreme spatial arrangement to be encountered. This is the transition state through which the "spinning motion" passes. Again, the barrier is low (1–2 kcal/mol) as long as the 2-phenylpyridine remains unsubstituted. However, a substituent R introduced into an *ortho* position of the phenyl ring not only destroys the symmetry of the latter but also significantly increases the barrier due to intramolecular *ortho*/*ortho′* repulsion in the coplanar transition state. Free rotation being impeded, we now have two enantiomeric conformers, one keeping the R group in the upper and the other in the lower hemisphere (Scheme 2). Thermal energy is required to overcome the barrier and to enable the "spinning motion" again.

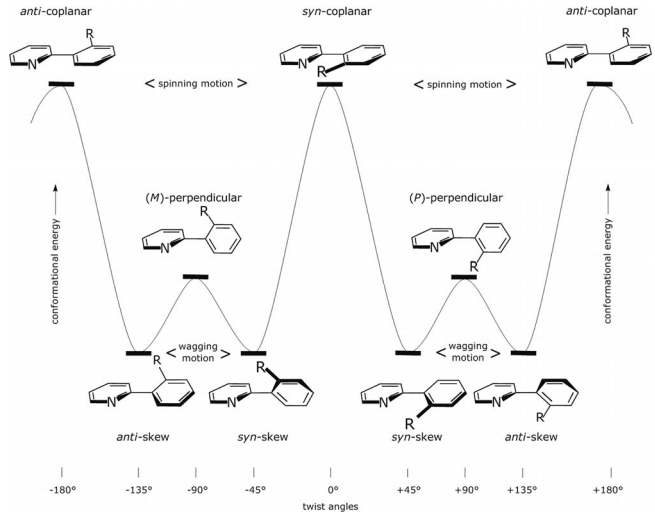

Scheme 2. Torsional energy diagram of 2-arylpyridines (*syn*- and *anti*-skew conformers being diastereoisomers, –45°/+45° *syn*-skew and –135°/+135° *anti*-skew conformers being enantiomers).

At first sight one might expect the *syn*-coplanar transition state alone to benefit significantly from the relief of crowding caused by the replacement of a stiff *ortho*-C–H bond by the deformable nitrogen lone pair. However, the free energy of the *anti*-coplanar transition state would be only marginally lower, that is, by half of the difference (1.0 kcal/mol) between the torsional barriers of biphenyl and 2-phenylpyridine. Such a simplistic assumption would neglect the nonrigidity of the 2-arylpyridine skeleton. Even if confined to coplanarity, it is distorted. The lengthening of the C(*ipso*)–C(*ipso′*) bond can be ignored in this context as it should be very similar in the biphenyl series. But the simultaneous introduction of a 2-aza ring member and a 2′-*ortho* substituent R causes the *para*–*ipso* and the *ipso′*–*para′* axes to bend out of collinearity (Scheme 3).

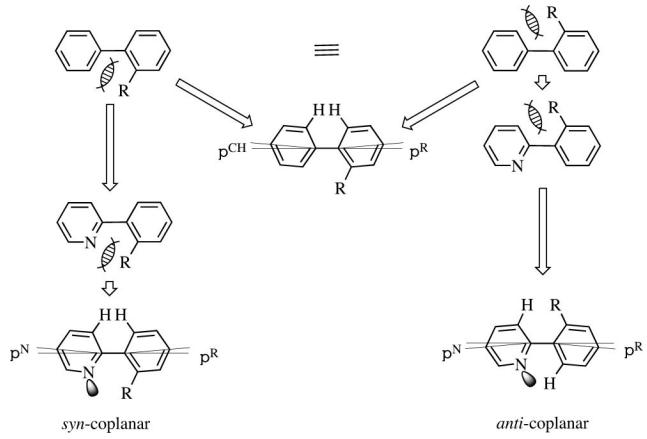

Scheme 3. Bending of the two (het)aromatic rings to minimize intramolecular steric repulsions in the coplanar torsional transition states.

The resulting curvature in the array of the two (het)aromatic rings minimizes the local intramolecular steric repulsions. Therefore the DFT energies of the *anti*-coplanar transition states are only slightly higher (0.5–1.7 kcal/mol) than those of the *syn*-coplanar transition states and are without exception considerably smaller than those of the carba-analogous conformers (e.g., 6.9 vs. 11.1 kcal/mol when R = isopropyl). *ortho*-Substituted biphenyls are equally subject to this out-of-collinearity distortion, but to a much lesser extent.

The calculated bend angles of the coplanar transition states are listed together with the DFT energies of the twisted ground and coplanar transition states (Table 4). The total out-of-collinearity distortion can be expressed as the sum of two bend angles, each of them being the sector encompassed by the *ipso–para* connecting line and the projection of the *ipso–ipso'* axis (see the thin lines in Scheme 3). The *ortho*-substituted ring pivots in such a way to increase the distance between its R group and the *ortho*-hydrogen atom facing the R group on the neighboring ring. The other (het)aromatic ring always moves in the same direction.

Conclusions

Due to the compressibility of the lone pair, the torsional barriers of the arylpyridines are up to 4.2 kcal/mol smaller than those of the carba-analogous biphenyls. Furthermore, the ground states of the 2-arylpyridines are less twisted than those of the biphenyls. Finally, due to an out-of-collinearity distortion, the intramolecular repulsion is attenuated in both rotational transition states, in the *syn* coplanar conformer (in which the pyridine nitrogen and the substituent R face each other) and in the *anti* coplanar conformer (in which they are on opposite sides of the molecule).

Experimental Section

General Methods: ^{1}H and ^{13}C NMR spectra of samples dissolved in deuteriochloroform were recorded at 400 and 100.6 MHz, respectively (Bruker Avance). Chemical shifts (δ) are given in ppm relative to the internal standard tetramethylsilane. IR spectra were recorded in chloroform solutions in the 4000–625 cm^{-1} frequency range, and mass spectra were obtained by electron impact fragmentation at an ionization potential of 70 eV with a source temperature of 200 °C (Thermo-Finnigan MAT 95XP).

The purity of all final products was testified by elemental analyses and gas chromatography using two capillary columns of different polarity [30 m × 0.35 mm × 0.25 μm DB 5MS (5% phenylmethylpolysiloxane) and 30 m × 0.35 mm × 0.25 μm DB23 (50% cyanopropylmethylpolysiloxane)]. Tetrahydrofuran and diethyl ether were stored over potassium hydroxide pellets in the presence of cuprous chloride, from which they were distilled, before being redistilled from sodium wire after the characteristic blue color of in situ generated sodium biphenyl ketyl (benzophenone-sodium "radical anion") had been found to persist. Pyridine was made anhydrous by azeotropic distillation with toluene. "Petroleum ether" refers to an alkane fraction with a boiling range of 40–60 °C. Air- and moisture-sensitive compounds were stored in Schlenk tubes or burettes. They were protected by and handled under an atmosphere of 99.995% pure nitrogen using appropriate glassware. Ethereal extracts were dried by using sodium sulfate if the product was isolated by distillation or crystallization. Silica gel of particle size 0.040–0.063 mm (230–400 mesh) was used for column chromatography.

Table 4. Relative DFT energies of the *syn*- and *anti*-skew ground states and the *syn*- and *anti*-coplanar transition states of 2-arylpyridines, and, in parentheses, the bend angles in the coplanar transition states.

Compound	R	DFT energy [kcal/mol] (Bend angle [°])			
		Z = N[a]		Z = CH[a]	
		anti-skew[b]	*syn*-coplanar[b]	*anti*-coplanar[b]	coplanar rel. to skew
1	H	0.0	0.4	0.4	2.0
			(–3.8)	(–3.8)[c]	(2.0)[c]
2[d]	CH_3	+0.6	3.1	3.6	7.1
			(+1.6)	(–9.1)[x]	(5.7)[d]
3[d]	CH_2CH_3	+0.8	3.4	4.6	8.5
			(+2.2)	(–9.1)[x]	(6.4)[d]
4	$CH(CH_3)_2$	+0.6	5.2	6.9	11.1
			(+3.4)	(–11.2)[x]	(7.9)[d]
5[d]	$C(CH_3)_3$	–[e]	9.0	10.6	15.1
			(+6.1)	(–13.5)[x]	(9.6)[d]

[a] Bend angles as defined in the text are given in parentheses. [b] DFT energies [B3LYP/6-311++G(2d,p) level] of the *syn*- and *anti*-skew and *syn*- and *anti*-coplanar conformers all of them relative to the *syn*-skew ground state. [c] The *syn*- and *anti*-skew conformers are identical. [d] Calculations on the corresponding compounds without the substituent at the 4-position. [e] The *anti*-skew conformer is not an energy minimum.

In general, the product-to-support ratio was approximately 1:20. The silica was suspended in petroleum ether and, as soon as all the air bubbles had escaped, was washed into the column. When the level of the liquid was still 3–5 cm above the layer of the solid, the dry powder, obtained by absorption of the dissolved crude product mixture onto a small volume (some 5–10 mL) of silica and subsequent evaporation to dryness, was poured onto the top of the column.

Preparation of 2-Arylpyridines 1–5

4-(Isopropyldimethylsilyl)pyridine: At –75 °C, butyllithium (13 mmol) in hexanes (7.8 mL) and chloro(isopropyl)dimethylsilane (1.8 g, 13 mmol) in diethyl ether (20 mL) were added consecutively to 4-bromopyridine (2.0 g, 13 mmol; set free from its commercial hydrochloride with saturated aqueous potassium carbonate, extracted with diethyl ether, and dried). After 45 min at 25 °C, the solvent was stripped off and the residue distilled; b.p. 55–57 °C/1 Torr; colorless oil; yield: 1.70 g (73%). ^{1}H NMR: δ = 8.54 (d, J = 5.6 Hz, 2 H), 7.35 (d, J = 5.6 Hz, 2 H), 0.95 (s, 7 H), 0.25 (s, 6 H) ppm. ^{13}C NMR: δ = 148.6 (2 C), 148.5, 128.7 (2 C), 17.3 (2 C), 13.2, –5.9 (2 C) ppm. MS: m/z (%) = 179 (22) $[M]^+$, 164 (3), 136 (100), 122 (10), 106 (18), 83 (41), 43 (23). $C_{10}H_{17}NSi$ (179.33): calcd. C 66.97, H 9.55, N 7.81; found C 67.05, H 9.91, N 7.92.

2-Chloro-4-(isopropyldimethylsilyl)pyridine: The compound was prepared analogously from 4-bromo-2-chloropyridine (2.5 g, 13 mmol); colorless liquid; b.p. 61–63 °C/1 Torr; yield: 1.92 g (69%). ^{1}H NMR: δ = 8.33 (dd, J = 7.8, 1.8 Hz, 1 H), 7.38 (t, J = 1.8 Hz, 1 H), 7.27 (dd, J = 9.5, 1.8 Hz, 1 H), 1.0 (m, 7 H), 0.27 (s, 6 H) ppm. ^{13}C NMR: δ = 153.1, 151.2, 148.5, 129.0, 127.0, 17.2 (2 C), 13.1, –5.9 (2 C) ppm. MS: m/z (%) = 213 (20) $[M]^+$, 172 (82), 170 (100), 156 (10), 93 (13), 83 (15), 43 (26). $C_{10}H_{16}ClNSi$ (213.78): calcd. C 56.18, H 7.54, N 6.55; found C 56.00, H 8.03, N 7.11.

2-Phenylpyridine (1): At –75 °C, phenyllithium (7.6 mmol) in dibutyl ether (4.2 mL) was added to pyridine (1.2 g, 15 mmol) in diethyl ether (15 mL). The cooling bath was removed and the mixture kept at 25 °C for 12 h. The solvent and excess of pyridine were evaporated at reduced pressure and the residue was eluted from silica gel (60 mL) with a 3:7 (v/v) mixture of diethyl ether and petroleum ether to give a colorless oil. Yield: 0.75 g (64%); b.p. 142–143 °C/15 Torr (Hickmann distillation, ref.[39–42] 140 °C/12 Torr); m.p. of the picrate 156–158 °C (ref.[39,40,42] m.p. 157 °C). ^{1}H NMR (200 MHz): δ = 8.73 (dd, J = 5.1, 0.6 Hz, 1 H), 8.0 (m, 2 H), 7.8 (m, 2 H), 7.5 (m, 3 H), 7.3 (m, 1 H) ppm.

4-(Isopropyldimethylsilyl)-2-(2-tolyl)pyridine (2): At –75 °C, *tert*-butyllithium (2.9 mmol) in pentanes (1.7 mL) and 4-(isopropyldimethylsilyl)pyridine (0.53 g, 3.0 mmol) were added consecutively to 2-bromotoluene (0.50 g, 2.9 mmol) in diethyl ether (10 mL). After 5 h at 25 °C the mixture was concentrated, absorbed onto a small quantity of silica gel, and dried before being poured into a chromatography column. Elution with a 1:4 (v/v) mixture of diethyl ether and petroleum ether mixture gave a colorless oil. Yield: 0.530 g, 67%. ^{1}H NMR: δ = 8.65 (d, J = 5.1 Hz, 1 H), 7.48 (s, 1 H), 7.4 (m, 1 H), 7.3 (m, 4 H), 2.36 (s, 3 H), 0.98 (br. s, 7 H), 0.28 (s, 6 H) ppm. $C_{17}H_{23}NSi$ (269.46): calcd. C 75.78, H 8.60, N 5.20; found C 75.68, H 8.66, N 5.38.

4-(Isopropyldimethylsilyl)-2-(2-ethylphenyl)pyridine (3): Compound **3** was prepared analogously from 1-bromo-2-ethylbenzene (0.50 g, 2.5 mmol) and 4-(isopropyldimethylsilyl)pyridine (0.20 g, 2.5 mmol) and obtained as a pale-yellow oil. Yield: 0.28 g (56%); b.p. 145–147 °C/1.4 Torr (Hickmann distillation). ^{1}H NMR: δ = 8.65 (dd, J = 4.8, 1.0 Hz, 1 H), 7.48 (t, J = 1.1 Hz, 1 H), 7.3 (m, 5 H), 2.71 (q, J = 7.5 Hz, 2 H), 1.12 (t, J = 7.5 Hz, 3 H), 0.98 (br. s, 7 H), 0.29 (s, 6 H) ppm. ^{13}C NMR: δ = 154.7, 148.6, 147.9, 141.9, 137.3, 129.7, 129.0, 128.9, 128.3, 126.6, 125.7, 26.0, 17.3 (2 C), 15.5, 13.3, –5.9 (2 C) ppm. MS: m/z (%) = 283 (93) $[M]^+$, 268 (4), 241 (47), 182 (100), 167 (10), 77 (10), 59 (20), 43 (6). $C_{18}H_{25}NSi$ (283.48): calcd. C 76.26, H 8.89; found C 75.98, H 9.20. HRMS (ESI): calcd. for $C_{18}H_{26}NSi$ $[M + H]^+$ 284.1845; found 284.1829.

2-(2-Isopropylphenyl)pyridine (4): At –75 °C, *tert*-butyllithium (2.7 mmol) in pentanes (1.6 mL) and pyridine (0.39 g, 4.9 mmol) were added consecutively to 2-bromoisopropylbenzene (0.50 g, 2.5 mmol) in diethyl ether (15 mL). The cooling bath was removed and the mixture was kept at 25 °C for 12 h. After the addition of water (25 mL), the organic phase was collected and dried, and the solvent was evaporated at reduced pressure. Chromatography of the residue on silica gel (eluent: 2:8 diethyl ether/petroleum ether mixture) gave a colorless oily product. Yield: 0.257 g, 52%; b.p. 102–105 °C/0.2 Torr (Hickmann distillation). ^{1}H NMR: δ = 8.68 (dt, J = 4.0, 0.8 Hz, 1 H), 7.73 (td, J = 7.7, 1.8 Hz, 1 H), 7.4 (m, 3 H), 7.3 (m, 3 H), 3.17 (sept., J = 6.9 Hz, 1 H), 1.19 (d, J = 6.9 Hz, 6 H) ppm. $C_{14}H_{15}N$ (197.28): calcd. C 85.24, H 7.66, N 7.10; found C 85.10, H 8.11, N 7.39.

The same product was obtained when a mixture of 2-bromopyridine (0.20 g, 1.3 mmol), 2-isopropylphenylboronic acid (0.27 g, 1.6 mmol), aq. 2.0 M potassium carbonate (1.3 mmol), and tetrakis(triphenylphosphane)palladium (0.047 g, 0.041 mmol) in benzene (10 mL) and ethanol (8.0 mL) was heated at 70 °C for 6 h. Upon chromatography (elution with a 3:7 mixture of diethyl ether and petroleum ether) a colorless oil exhibiting all properties of compound **4** was isolated (yield: 0.230 g, 92%).

4-(Isopropyldimethylsilyl)-2-(2-*tert*-butylphenyl)pyridine (5): Compound **5** was obtained from 4-(isopropyldimethylsilyl)pyridine (1.7 g, 5.6 mmol) and 1-bromo-2-*tert*-butylbenzene (1.0 g, 4.7 mmol). Chromatography of the crude brown oil (elution with a 1:4 diethyl ether and petroleum ether mixture) allowed to collect a first fraction consisting of a mixture of 2-*tert*-butyl-4-(isopropyldimethylsilyl)- and 2-[(2-*tert*-butyl)phenyl]-4-(isopropyldimethylsilyl)-pyridine in an approximately 1:1 molar ratio. Two subsequent chromatographic fractions contained unreacted 4-(isopropyldimethylsilyl)pyridine (0.35 g) and 4,4′-bis(isopropyldimethylsilyl)-2,2′-bipyridine (0.14 g), respectively. The expected product was separated as a pale-yellow oil (0.042 g, 2.9%) by semi-preparative HPLC of the first fraction after elution with a 90:10 (v/v) mixture of acetonitrile/water mixture using a C18 column. ^{1}H NMR: δ = 8.57 (d, J = 4.8 Hz, 1 H), 7.55 (dd, J = 8.0, 0.9 Hz, 1 H), 7.40 (d, J = 0.9 Hz, 1 H), 7.3 (m, 2 H), 7.22 (td, J = 7.5, 1.0 Hz, 1 H), 7.10 (dd, J = 7.5, 1.5 Hz, 1 H), 1.17 (s, 9 H), 0.95 (br. s, 7 H), 0.26 (s, 6 H) ppm. ^{13}C NMR: δ = 162.0, 148.0, 147.7, 146.8, 141.1, 131.4, 129.9, 127.8, 126.8, 126.6, 125.1, 36.4, 32.3 (3 C), 17.3 (2 C), 13.3, –5.9 (2 C) ppm. MS: m/z (%) = 311 (38) $[M]^+$, 296 (65), 268 (7), 238 (21), 210 (100), 73 (27), 57 (31). $C_{20}H_{29}NSi$ (311,54): calcd. C 77.11, H 9.38, N 4.50; found C 77.00, H 9.56, N 4.57. When 2-chloro-4-(dimethylisopropylsilyl)pyridine was treated with 2-*tert*-butylphenylboronic acid in the presence of tetrakis(triphenylphosphane)palladium under Suzuki–Miyaura conditions[43] a complex mixture of products was obtained. Only traces of the expected product were detected by GC–MS analysis.

Variable-Temperature NMR Spectroscopy: NMR spectra were recorded by using a spectrometer operating at a field of 14.4 T (600 MHz for ^{1}H) (Varian INOVA). The variable-temperature experiments of compound **5** were performed in $CDFCl_2$ whereas the spectra of compounds **2**–**4** were recorded in a $CHF_2Cl/CHFCl_2/C_6D_6$ mixture (9:3:1, v/v). The NMR tubes containing the compounds were prepared by using a vacuum line. First a small amount

(50 μL) of hexadeuteriobenzene was introduced by means of a microsyringe for locking purposes (this step was not necessary for the sample of **5**). The NMR tube was then immersed in liquid nitrogen and evacuated to condense about 0.45 mL of chlorodifluoromethane (Freon 22) and about 0.15 mL of dichlorofluoromethane (Freon 21) transferred as gases from lecture bottles (in the case of compound **5**, 0.65 mL of $CDFCl_2$ was transferred). The tubes were subsequently sealed under reduced pressure (0.01 mbar) by using a methane/oxygen torch. Avoiding any rapid temperature change, the samples were cautiously warmed to 25 °C, at which the Freons develop a pressure of about 8 atm. After a few hours at ambient temperature, the samples could be safely introduced into the probe head of the spectrometer, already cooled to –30 °C. Low-temperature 600 MHz ^{1}H NMR spectra (compounds **2**–**5**) were acquired without spinning using a 5 mm dual direct probe with a 9000 Hz sweep width, 2.0 μs (20° tip angle) pulse width, 3 s acquisition time, and 1 s delay time. A shifted sine bell weighting function[44] equal to the acquisition time (i.e., 3 s) was applied before the Fourier transformation. Usually 32–64 scans were collected. Low-temperature 150.8 MHz ^{13}C NMR spectra (compounds **2**, **4**, and **5**) were acquired without spinning and under proton decoupling conditions with a 38000 Hz sweep width, 4.2 μs (60° tip angle) pulse width, 1 s acquisition time, and 1 s delay time. A line-broadening function of 1–2 Hz was applied before the Fourier transformation. Usually 128–512 scans were collected.

When operating the NMR apparatus at low temperature, a flow of dry nitrogen was first passed through a precooling unit adjusted to –50 °C. Then the gas entered an inox steel heat-exchanger immersed in liquid nitrogen and connected to the NMR probe head by a vacuum-insulated transfer line. Gas flows of 10–30 L min^{-1} were required to descend to the desired temperature. Temperature calibrations were performed before the experiments by using a digital thermometer and a Cu/Ni thermocouple placed in an NMR tube filled with isopentane. The conditions were kept as identical as possible in all subsequent work. In particular, the sample was not spun and the gas flow was the same as that used during the acquisition of the spectra. The uncertainty in temperature measurements can be estimated as ±2 °C.

Line-shape simulations were performed by using a PC version of the QCPE DNMR6 program.[45] Electronic superimposition of the original and simulated spectra enabled the determination of the most reliable rate constant. The rate constants thus obtained at various temperatures afforded the free energy of activation $\Delta G^{\neq}$ for bond rotation by use of the Eyring equation.[46] In all cases investigated, the activation energy $\Delta G^{\neq}$ was found to be virtually invariant in the given temperature range, thus implying a negligible activation entropy $\Delta S^{\neq}$.[47]

Computational Work: A complete conformational search was preliminarily carried out with the molecular mechanics force field (MMFF) using the Monte-Carlo method implemented in the TITAN 1.0.5 package.[48] The most stable conformers thus identified were subsequently energy-minimized by DFT computations. These were performed by using the Gaussian 09 program[49] on Xeon® servers, the operating system being the Red Hat Enterprise Linux 5.5, using the standard geometry optimization included in Gaussian 09.[50] All the calculations employed the B3LYP hybrid HF-DFT method[51] and the 6-311++G(2d,p) basis set. Harmonic vibrational frequencies were calculated for all stationary points. As revealed by the frequency analysis, imaginary frequencies were absent in all ground states whereas just one imaginary frequency was associated with each transition state. Visual inspection of the corresponding normal modes[52] validated the identification of the transition states. The energy values listed in Tables 2 and 4 represent total electronic energies. In general, it was shown that these give the best fit with experimental dynamic NMR spectroscopic data.[53] Therefore the computed values were not corrected for zero-point energy contributions or other thermodynamic parameters. This avoids artifacts that might result from the ambiguous choice of reference temperature, empirical scaling factors,[54] and idealization of low-frequency vibrators as harmonic oscillators, which cause difficulties in the correct evaluation of the entropic contribution.[55,56]

Supporting Information (see footnote on the first page of this article): Variable-temperature NMR spectra of **4**, computational data for **2**–**5** and their carba-analogues, and NMR spectra of **2**–**5** and their precursors.

Acknowledgments

The authors are grateful to the University of Bologna (RFO funds 2009), the Ministero dell′Università e Ricerca, Roma (MUR PRIN 2008 prot. 2008LYSEBR-004), and the Schweizerische Nationalfonds zur Förderung der wissenschaftlichen Forschung, Bern (grant 20-100′336-02) for financial support. They are particularly indebted to Dr. E. Solari of the EPFL-ISIC Analytical Services, Lausanne, and REDOX, Monza, Italy, for the elemental analyses of **2**–**4**.

[1] R. J. Gillespie, *Angew. Chem.* **1967**, *79*, 885–896; *Angew. Chem. Int. Ed. Engl.* **1967**, *6*, 819–830.
[2] M. Schlosser, *Structure and Reactivity of Polar Organometallic Compounds*, Springer, Berlin, **1973**.
[3] M. Charton, *Top. Curr. Chem.* **1983**, *114*, 57–91.
[4] A. Bondi, *J. Phys. Chem.* **1964**, *68*, 441–451.
[5] R. Gallo, *Prog. Phys. Org. Chem.* **1983**, *14*, 115–163.
[6] D. R. Lide, *J. Chem. Phys.* **1957**, *27*, 343–352.
[7] M. D. Harmony, M. V. Laurie, R. L. Kuczkowski, R. H. Schwedenman, D. A. Ramsay, F. L. Lovas, W. J. Lafferty, A. G. Maki, *J. Phys. Chem. Ref. Data* **1979**, *8*, 619–721.
[8] P. George, J. P. Glusker, C. W. Bock, *THEOCHEM* **1995**, *338*, 155–173.
[9] K. Tagaki, T. Kojima, *J. Phys. Soc. Jpn.* **1971**, *30*, 1145–1157.
[10] K. S. Pitzer, *Discuss. Faraday Soc.* **1951**, *10*, 66–73.
[11] F. A. L. Anet, I. Yavari, *J. Am. Chem. Soc.* **1977**, *99*, 2794–2796.
[12] N. A. Allinger, J. G. D. Carpenter, F. M. Karkowski, *J. Am. Chem. Soc.* **1965**, *87*, 1232–1236.
[13] J. E. Parkin, P. J. Buckley, C. C. Costain, *J. Mol. Spectrosc.* **1981**, *89*, 465–483.
[14] K. D. Dobbs, K. Sohlberg, *J. Chem. Theory Comput.* **2006**, *2*, 1530–1537.
[15] O. Bastiansen, *Acta Chem. Scand.* **1949**, *3*, 408–414.
[16] A. Almenningen, O. Bastiansen, L. Fernholt, B. N. Cyvin, S. J. Cyvin, S. Sandal, *J. Mol. Struct.* **1985**, *128*, 59–76.
[17] M. P. Johansson, J. Olsen, *J. Chem. Theory Comput.* **2008**, *4*, 1460–1471.
[18] F. Grein, *J. Phys. Chem. A* **2002**, *106*, 3823–3827.
[19] D. Gust, M. W. Fagan, *J. Org. Chem.* **1980**, *45*, 2511–2512.
[20] H. Förster, F. Vögtle, *Angew. Chem.* **1977**, *89*, 443–455; *Angew. Chem. Int. Ed. Engl.* **1977**, *16*, 429–441.
[21] F. Vögtle, *Cyclophane Chemistry*, Wiley, Chichester, **1993**.
[22] S. Fujita, H. Nozaki, *Bull. Chem. Soc. Jpn.* **1971**, *44*, 2827–2833.
[23] S. Fujita, S. Hirano, H. Nozaki, *Tetrahedron Lett.* **1972**, *13*, 403–406.
[24] R. Annunziata, M. Benaglia, F. Cozzi, A. Mazzanti, *Chem. Eur. J.* **2009**, *15*, 4373–4381.
[25] M. Benaglia, F. Cozzi, M. Mancinelli, A. Mazzanti, *Chem. Eur. J.* **2010**, *16*, 7456–7468.

[26] J. R. Fletcher, I. O. Sutherland, *J. Chem. Soc. C* **1969**, 1504–1505.
[27] F. Vögtle, A. H. Effler, *Chem. Ber.* **1969**, *102*, 3071–3076.
[28] F. Vögtle, P. Neumann, *Chimia* **1972**, *26*, 64–70.
[29] S. A. Sherrod, R. L. Da Costa, R. A. Barnes, V. Boekelheide, *J. Am. Chem. Soc.* **1974**, *96*, 1565–1577.
[30] V. Boekelheide, K. Galuszko, K. S. Szeto, *J. Am. Chem. Soc.* **1974**, *96*, 1578–1581; L. H. Weaver, B. W. Matthews, *J. Am. Chem. Soc.* **1974**, *96*, 1581–1584.
[31] R. Ruzziconi, S. Spizzichino, L. Lunazzi, A. Mazzanti, M. Schlosser, *Chem. Eur. J.* **2009**, *15*, 2645–2652.
[32] A. Mazzanti, L. Lunazzi, R. Ruzziconi, S. Spizzichino, M. Schlosser, *Chem. Eur. J.* **2010**, *16*, 9186–9192.
[33] R. Ruzziconi, S. Spizzichino, A. Mazzanti, L. Lunazzi, M. Schlosser, *Org. Biomol. Chem.* **2010**, *8*, 4463–4471.
[34] a) A. Mazzanti, L. Lunazzi, M. Minzoni, J. E. Anderson, *J. Org. Chem.* **2006**, *71*, 5474–5481; b) L. Lunazzi, A. Mazzanti, M. Minzoni, *J. Org. Chem.* **2006**, *71*, 9297–9301.
[35] The aryl–aryl rotation barriers were found to be independent, within experimental error, of the type of diastereotopicity probe bonded to the *meta* position.[31,34a] Also, calculations predict essentially the same barrier for compounds with or without such a *meta* substituent. For instance, our DFT computations predict that 2-isopropylbiphenyl has an aryl–aryl rotation barrier of 11.0 kcal/mol. When a 3′ diastereotopicity probe is included in these calculations the barrier is 11.1 kcal/mol.[34a]
[36] K. Ziegler, K. Zeiser, *Ber. Dtsch. Chem. Ges.* **1930**, *63*, 1847–1851.
[37] K. Ziegler, K. Zeiser, *Justus Liebigs Ann. Chem.* **1931**, *485*, 174–192.
[38] The 4-position on pyridine corresponds to the 3′-position of a 2-substituted 1,1′-biphenyl.
[39] J. Overhoff, G. G. Tilman, *Recl. Trav. Chim. Pays-Bas* **1929**, *48*, 993–996.
[40] K. Ziegler, K. Zeiser, *Ber. Dtsch. Chem. Ges.* **1930**, *63*, 1847–1851.
[41] J. C. V. Evans, C. F. H. Allen, *Org. Synth.* **1943**, *2*, 517–519.
[42] T. Kato, H. Yamanaka, T. Adachi, H. Hiranuma, *J. Org. Chem.* **1967**, *32*, 3788–3790.
[43] C. M. So, C. P. Lau, F. Y. Kwong, *Org. Lett.* **2007**, *9*, 2795–2798.
[44] T. D. W. Claridge, *High-Resolution NMR Techniques in Organic Chemistry*, Pergamon Press, Oxford, **1999**, p. 71.
[45] J. H. Brown, C. H. Bushweller, *DNMR6*: *Calculation of NMR Spectra Subject to the Effects of Chemical Exchange (program 633)*, *QCPE Bull.*, Bloomington, Indiana, **1983**, vol. 3, pp. 103–103. A copy of the program is available on request from the authors (L.L. and A.M.)
[46] H. Eyring, *Chem. Rev.* **1935**, *17*, 65–77.
[47] L. Lunazzi, M. Mancinelli, A. Mazzanti, *J. Org. Chem.* **2007**, *72*, 5391–5394; D. Casarini, L. Lunazzi, A. Mazzanti, *Eur. J. Org. Chem.* **2010**, *75*, 2035–2056.
[48] *TITAN 1.0.5*, Wavefunction, Inc., Irvine, CA.
[49] M. J. Frisch, G. W. Trucks, H. B. Schlegel, G. E. Scuseria, M. A. Robb, J. R. Cheeseman, G. Scalmani, V. Barone, B. Mennucci, G. A. Petersson, H. Nakatsuji, M. Caricato, X. Li, H. P. Hratchian, A. F. Izmaylov, J. Bloino, G. Zheng, J. L. Sonnenberg, M. Hada, M. Ehara, K. Toyota, R. Fukuda, J. Hasegawa, M. Ishida, T. Nakajima, Y. Honda, O. Kitao, H. Nakai, T. Vreven, J. A. Montgomery Jr., J. E. Peralta, F. Ogliaro, M. Bearpark, J. J. Heyd, E. Brothers, K. N. Kudin, V. N. Staroverov, R. Kobayashi, J. Normand, K. Raghavachari, A. Rendell, J. C. Burant, S. S. Iyengar, J. Tomasi, M. Cossi, N. Rega, J. M. Millam, M. Klene, J. E. Knox, J. B. Cross, V. Bakken, C. Adamo, J. Jaramillo, R. Gomperts, R. E. Stratmann, O. Yazyev, A. J. Austin, R. Cammi, C. Pomelli, J. W. Ochterski, R. L. Martin, K. Morokuma, V. G. Zakrzewski, G. A. Voth, P. Salvador, J. J. Dannenberg, S. Dapprich, A. D. Daniels, O. Farkas, J. B. Foresman, J. V. Ortiz, J. Cioslowski, D. J. Fox, *Gaussian 09, Revision A.02*, Gaussian, Inc., Wallingford, CT, **2009**.
[50] C. Peng, P. Y. Ayala, H. B. Schlegel, M. J. Frisch, *J. Comput. Chem.* **1996**, *17*, 49–56.
[51] C. Lee, W. Yang, R. G. Parr, *Phys. Rev. B* **1988**, *37*, 785–789; A. D. Becke, *J. Chem. Phys.* **1993**, *98*, 5648–5652; P. J. Stephens, F. J. Devlin, C. F. Chabalowski, J. M. Frisch, *J. Phys. Chem.* **1994**, *98*, 11623–11627.
[52] *GaussView 5.0.9*, Gaussian, Inc., Wallingford, CT, **2009**.
[53] P. Y. Ayala, H. B. Schlegel, *J. Chem. Phys.* **1998**, *108*, 2314–2325.
[54] C. F. Tormena, R. Rittner, R. J. Abraham, E. A. Basso, B. C. Fiorin, *J. Phys. Org. Chem.* **2004**, *17*, 42–48.
[55] M. W. Wong, *Chem. Phys. Lett.* **1996**, *256*, 391–399.
[56] S. E. Wheeler, A. J. McNeil, P. Müller, T. M. Swager, K. N. Houk, *J. Am. Chem. Soc.* **2010**, *132*, 3304–3311.

Received: July 12, 2011
Published Online: September 27, 2011

